RECENT KLOE RESULTS ON HADRON PHYSICS*

Paolo Gauzzi

on behalf of the KLOE-2 Collaboration

Università di Roma "La Sapienza" e INFN Sezione di Roma
P.le A. Moro 5, 00185 Rome, Italy
paolo.gauzzi@roma1.infn.it

(Received June 9, 2014)

Recent KLOE results concerning the $\eta \to 3\pi$ decay, the Dalitz decays $\phi \to \eta e^+e^-$ and $\phi \to \pi^0 e^+e^-$, and the η and $\pi^0\pi^0$ production in $\gamma\gamma$ collisions are reported. Prospects for the KLOE-2 data-taking are also presented.

DOI:10.5506/APhysPolBSupp.7.425
PACS numbers: 13.25.Jx, 13.66.Bc, 13.66.Jn

1. Introduction

The KLOE Collaboration took data from 2001 to 2006 at the Frascati ϕ-factory DAΦNE, collecting about 2.5 fb^{-1} at the peak of the $\phi(1020)$, and 250 pb^{-1} off-peak, mainly at $\sqrt{s} = 1$ GeV. In 2008, a new interaction scheme for DAΦNE has been tested, aiming to an increase of a factor of three in luminosity. Following this test, a new data-taking campaign of the KLOE experiment (KLOE-2 in the following) with an upgraded detector has been proposed [1]. The DAΦNE commissioning started in 2010, but hardware failures lead to a long shutdown of the machine. The commissioning has been resumed at the end of 2011. The installation of the new detectors in KLOE started in December 2012 and completed in July 2013.

1.1. The KLOE-2 upgrade

As a first step of the detector upgrade, a tagger system for scattered electrons in $\gamma\gamma$ processes has been installed in 2010 before the start of the commissioning. It consists of two different devices: *(i)* the Low Energy Tagger

* Presented at "Excited QCD 2014", Bjelašnica Mountain, Sarajevo, Bosnia and Herzegovina, February 2–8, 2014.

(LET) placed close to the interaction point (IP), made of two calorimeters of LYSO crystals readout by SiPM, to detect electrons with energy between 130 and 300 MeV; *(ii)* the High Energy Tagger (HET) for electrons with $E > 400$ MeV, made of two scintillator hodoscopes readout by PMT, symmetrically placed 11 m far from the IP, after the first bending dipoles of DAΦNE.

During the last shutdown, an Inner Tracker made of four layers of cylindrical triple GEM has been installed between the beam-pipe and the Drift Chamber, to improve the resolution for decay vertices close to the IP, and to increase the acceptance for low momentum tracks. Moreover, two Crystal Calorimeters (CCALT) have been added to cover the low polar angle regions to increase the acceptance for γ and $e^{\pm}$, originating from the IP, down to 10°, and finally the DAΦNE focusing quadrupoles have been instrumented with calorimeters (QCALT) made of tungsten and scintillator tiles.

2. $\eta \to \pi^+\pi^-\pi^0$

The $\eta \to 3\pi$ decay is isospin violating, and it is mainly induced by a QCD Lagrangian term proportional to the d and u quark mass difference. Once the amplitude for this decay is known, the measurement of the decay rate is suitable for a precise determination of the ratio of the light quark masses $Q^2 = \frac{m_s^2 - \hat{m}^2}{m_d^2 - m_u^2}$, where $\hat{m} = \frac{1}{2}(m_d + m_u)$. The Dalitz plot of $\eta \to \pi^+\pi^-\pi^0$ is described in terms of $X = \sqrt{3}\frac{E_+ - E_-}{\Delta}$ and $Y = 3\frac{E_0 - m_0}{\Delta} - 1$ with $\Delta = m_\eta - 2m_\pm - m_0$, and is usually parametrized as a power expansion around its centre ($X = Y = 0$), $|A(X,Y)|^2 = 1 + aY + bY^2 + cX + dX^2 + eXY + fY^3$.

KLOE collected about 100 millions of η mesons produced in the radiative decay $\phi \to \eta\gamma$, easily identified by the recoil photon of $E = 363$ MeV. By using a subsample of 450 pb^{-1} of data, we already measured the parameters of the Dalitz plot [2]. This result has been used in two different dispersive approaches to obtain the Q ratio and then the light quark masses [3, 4].

A new analysis of this decay based on much more statistics has been performed in order to reduce the systematic uncertainties on the parameters. A data sample of 1.7 fb^{-1} has been processed with a different analysis scheme, by replacing the kinematic fit with constraints from two-body decay kinematics, and with an improved Monte Carlo (MC) simulation. In Table I, the preliminary results of the new fit are compared to the old ones: the new parameters agree within the uncertainties with the old results, the C-violating parameters c and e are consistent with zero as expected, and the need of the f parameter to fit the Dalitz plot is confirmed. The systematic uncertainties are still under evaluation.

TABLE I

Parameters of the Dalitz plot of $\eta \to \pi^+\pi^-\pi^0$.

	Old analysis	New analysis (prelim.)
a	$-1.090 \pm 0.005^{+0.008}_{-0.019}$	-1.103 ± 0.003
b	$0.124 \pm 0.006 \pm 0.010$	0.1419 ± 0.0029
d	$0.057 \pm 0.006^{+0.007}_{-0.016}$	0.0725 ± 0.0027
f	$0.14 \pm 0.01 \pm 0.02$	0.154 ± 0.006
$P(\chi^2)$	73%	27%

3. Transition Form Factors

The Transition Form Factors (TFFs) describe the coupling of mesons to photons and provide information about the nature of the mesons and their structure. Recently, the interest in the TFFs has been renewed since they are an essential ingredient in the calculation of the hadronic Light-by-Light (LbL) scattering contribution to the anomalous magnetic moment of the muon [5]. The leading contribution to the LbL scattering is the single pseudoscalar exchange (Fig. 1). The calculation of this contribution is model dependent since the exchanged meson is off-shell, and the TFFs for off-shell meson are not measurable quantities. Nevertheless, any experimental information the TFFs, both for space-like and time-like q^2, can help in constraining the models used in the calculations. The TFFs at time-like q^2 can be studied by means of the Dalitz decays, like $\phi \to \eta e^+e^-$ and $\phi \to \pi^0 e^+e^-$, while $\gamma\gamma$ processes can be exploited to access space-like q^2.

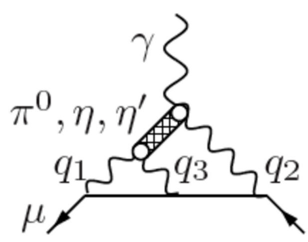

Fig. 1. Dominant contribution to the hadronic LbL scattering contribution to $(g-2)_\mu$.

The TFFs measured in Dalitz decays are functions of the four-momentun squared $q^2 = m^2_{\ell^+\ell^-}$, and according to the Vector Meson Dominance (VMD) are usually parametrized as $F(q^2) = 1/(1 - \frac{q^2}{\Lambda^2})$, where Λ is a characteristic mass, identified with the nearest vector meson. The dilepton invariant mass distributions of $\eta \to e^+e^-\gamma$ and $\eta \to \mu^+\mu^-\gamma$, measured by NA60 [6] and by the A2 Collaboration at MAMI [7, 8], are described by $\Lambda_\eta^{-2} = 1.92 \div 1.95$ GeV^{-2} in agreement with the VMD predictions $\Lambda_\eta^{-2} = 1.88$ GeV^{-2}, while the TFF of $\omega \to \pi^0\mu^+\mu^-$, also measured by NA60, gives $\Lambda_\omega^{-2} = 2.24$ GeV^{-2} in disagreement with the VMD prediction 1.68 GeV^{-2}. To explain this behaviour, other models have been proposed [9–11] that predict deviations from VMD also for $\phi \to \eta(\pi^0)\ell^+\ell^-$.

3.1. $\phi \to \eta e^+e^-$

Before the KLOE analysis, there was only one low statistics measurement by SND, $\Lambda_\phi^{-2} = (3.8 \pm 1.8)$ GeV^{-2}, to be compared with the VMD expectation $\Lambda_\phi^{-2} \simeq m_\phi^{-2} \simeq 1$ GeV^{-2}. We analysed 1.7 fb^{-1} of data looking for $\phi \to \eta e^+e^-$ with $\eta \to \pi^0\pi^0\pi^0$. The $m_{e^+e^-}$ distribution is shown in Fig. 2. From the event counting, we obtain $\mathrm{Br}(\phi \to \eta e^+e^-) = (1.075 \pm 0.007 \pm 0.038) \times 10^{-4}$. The slope $b = \Lambda_\phi^{-2}$ is extracted from a fit of the distribution of the e^+e^- invariant mass to the parametrization from Ref. [12], by using the one-pole formula for the TFF. We obtain a value, $b = (1.17 \pm 0.10^{+0.07}_{-0.11})$ GeV^{-2}, which is consistent with the VMD predictions.

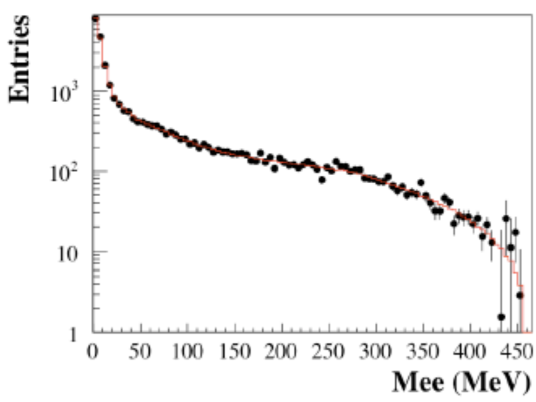

Fig. 2. e^+e^- invariant mass for $\phi \to \eta e^+e^-$.

3.2. $\phi \to \pi^0e^+e^-$

The Dalitz decay $\phi \to \pi^0e^+e^-$ has been measured by the Novosibirsk experiments CMD-2 and SND, that reported $\mathrm{Br}(\phi \to \pi^0e^+e^-) = (1.22 \pm 0.34 \pm 0.21) \times 10^{-5}$ and $(1.01 \pm 0.28 \pm 0.29) \times 10^{-5}$, respectively. Up to now, there are no data available on the TFFs slope.

In the sample of 1.7 fb^{-1}, we selected about 9000 events for this decay. In Fig. 3 the data-MC comparison is shown for the e^+e^- invariant mass. The residual background, mainly coming from radiative Bhabha scattering, is subtracted by fitting the distribution of the recoil mass against the e^+e^- pair. The subtracted invariant mass distribution is shown in Fig. 4. The points refer to data, and the solid histogram is the MC simulation assuming point-like particles (FF = 1). The extraction of the TFF from the ratio of those two distributions and the evaluation of the branching ratio are in progress.

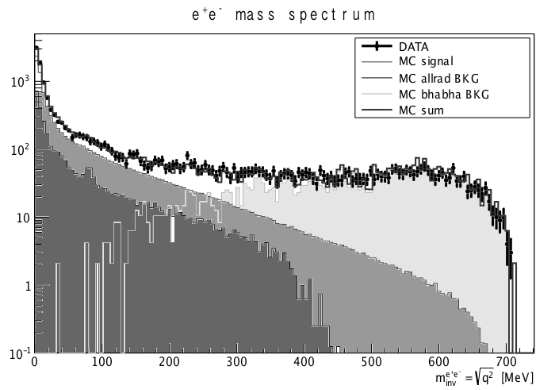

Fig. 3. e^+e^- invariant mass distribution for $\phi \to \pi^0 e^+e^-$ candidate events.

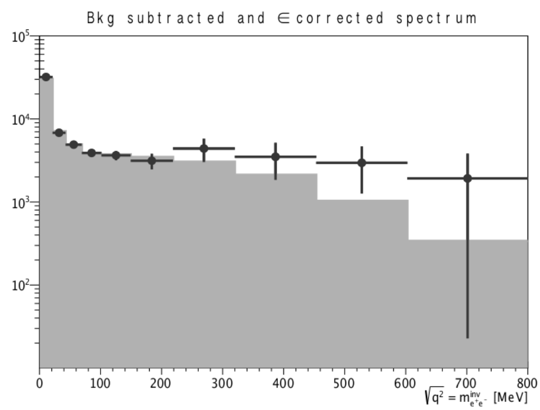

Fig. 4. Invariant mass after background subtraction (points = data, solid histogram = MC with FF = 1).

3.3. $\gamma\gamma \to \eta$

With the KLOE data, we measured the two-photon width of the η meson by detecting events $e^+e^- \to e^+e^-\eta$, with $\eta \to \pi^+\pi^-\pi^0$ and $\pi^0\pi^0\pi^0$. The scattered leptons were not detected because the taggers were not present, then in order to avoid the large background from ϕ decays, we analysed the 250 pb^{-1} collected at $\sqrt{s} = 1$ GeV. In Figs. 5–6 the distributions of the missing mass with respect to $\pi^+\pi^-\pi^0$ and $\pi^0\pi^0\pi^0$, respectively, are shown. By fitting these histograms, we obtained the cross sections $\sigma(e^+e^- \to e^+e^-\eta) = (34.5 \pm 2.5 \pm 1.3)$ pb and $\sigma(e^+e^- \to e^+e^-\eta) = (32.0 \pm 1.5 \pm 0.9)$ pb for the charged and neutral η decay channel, respectively. By combining them, $\sigma(e^+e^- \to e^+e^-\eta) = (32.7 \pm 1.3 \pm 0.7)$ pb, from which we extract the most precise measurement to date of the two-photon width: $\Gamma(\eta \to \gamma\gamma) = (520 \pm 20 \pm 13)$ eV [13].

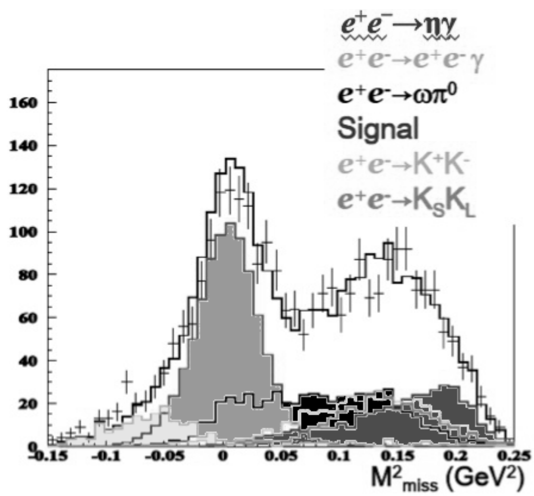

Fig. 5. $\gamma\gamma \to \eta \to \pi^+\pi^-\pi^0$.

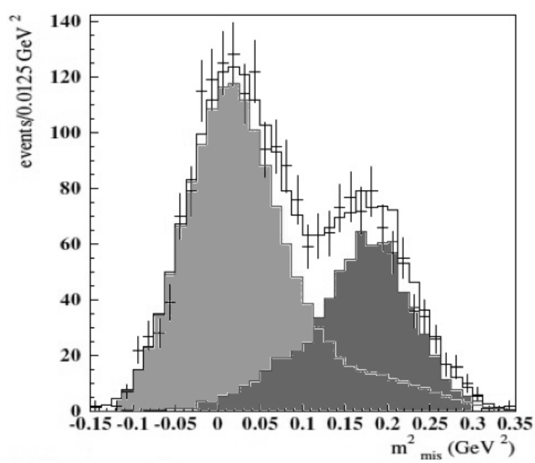

Fig. 6. Dark grey: $\gamma\gamma \to \eta \to \pi^0\pi^0\pi^0$; light grey: $e^+e^- \to \eta\gamma$ with $\eta \to \pi^0\pi^0\pi^0$.

3.4. $\gamma\gamma \to \pi^0$

At KLOE-2, we plan to measure $\Gamma(\pi^0 \to \gamma\gamma)$, which is presently known with 2.8% accuracy after the measurement by the PrimEx Collaboration. We will run mostly at the peak of the ϕ, and by detecting the two scattered leptons in the HET, we will select $e^+e^- \to e^+e^-\pi^0$ with quasi-real photons ($q^2 \simeq 0$). We expect to collect about 10 000 events in 5 fb^{-1} of data, in order to reach a 1% accuracy in $\Gamma(\pi^0 \to \gamma\gamma)$. Moreover, we plan to measure the $\pi^0\gamma^*\gamma$ TFF with a quasi-real photon, $q^2 \simeq 0$, and a virtual one, $|q^2| < 0.1$ GeV^2, by selecting events in which one electron is detected in the HET and the other at large angle in the KLOE main detector. This is a still unexplored q^2 region, important to check the TFF parametrizations.

3.5. $\gamma\gamma \to \pi^0\pi^0$

In the off-peak data sample, we selected $e^+e^- \to e^+e^-\pi^0\pi^0$ by looking at events with only four prompt photons. This process is interesting to study the production of the lowest mass scalar meson $f_0(500)$, but it is also important for the new dispersive approach proposed for the LbL scattering [14]. In Fig. 7, it is shown the four photon invariant mass distribution; there is a clear excess of events, with respect to all known background sources, at low mass values. The residual background is still under study. The next step will be the measurement of the $e^+e^- \to e^+e^-\pi^0\pi^0$ cross section.

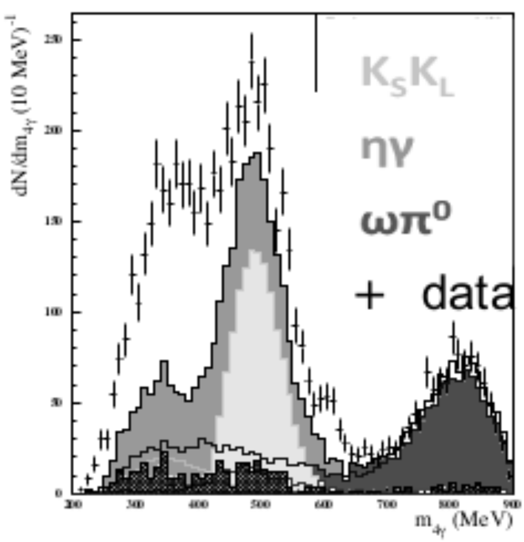

Fig. 7. Four photon invariant mass for $e^+e^- \to e^+e^-\pi^0\pi^0$, the top solid histogram is the sum of all the background processes.

At KLOE-2, the detection of the scattered electrons will help in reducing the background due to the possibility to close the kinematics of the events. The relevant energy region can be covered by selecting events with either HET–HET or HET–LET coincidences.

REFERENCES

[1] G. Amelino-Camelia *et al.*, *Eur. Phys. J.* **C68**, 619 (2010).
[2] F. Ambrosino *et al.*, *J. High Energy Phys.* **0805**, 006 (2008).
[3] G. Colangelo, S. Lanz, E. Passemar, *PoS* **CD09**, 047 (2009).
[4] K. Kampf, M. Knecht, J. Novotny, M. Zdrahal, *Phys. Rev.* **D84**, 114015 (2011).
[5] F. Jegerlehner, A. Nyffeler, *Phys. Rep.* **477**, 1 (2009).
[6] A. Uras, *J. Phys. Conf. Ser.* **270**, 012038 (2011).
[7] H. Berghauser *et al.*, *Phys. Lett.* **B701**, 562 (2011).
[8] P. Aguar-Bartolome *et al.*, *Phys. Rev.* **C89**, 044608 (2014).
[9] C. Terschlusen, S. Leupold, *Prog. Part. Nucl. Phys.* **67**, 401 (2012).
[10] S.P. Schneider, B. Kubis, F. Niecknig, *Phys. Rev.* **D86**, 054013 (2012).
[11] S. Ivashyn, *Probl. Atomic Sci. Technol.* **2012N1**, 179 (2012).
[12] L. Landsberg, *Phys. Rep.* **128**, 301 (1985).
[13] D. Babusci *et al.*, *J. High Energy Phys.* **1301**, 119 (2013).
[14] G. Colangelo *et al.*, `arXiv:1402.7081 [hep-ph]`.